



**KTH Industrial Engineering
and Management**

Adhesion in the wheel–rail contact

Yi Zhu

Doctoral thesis
Department of Machine Design
Royal Institute of Technology
SE-100 44 Stockholm

TRITA – MMK 2013: 15
ISSN 1400-1179
ISRN/KTH/MMK/R-13/15-SE
ISBN 978-91-7501-896-6

TRITA – MMK 2013:15
ISSN 1400-1179
ISRN/KTH/MMK/R-13/15-SE
ISBN 978-91-7501-896-6
Adhesion in the wheel–rail contact

Yi Zhu, yiz@kth.se

Doctoral thesis

Academic thesis, which with the approval of Kungliga Tekniska Högskolan, will be presented for public review in fulfillment of the requirements for a Doctoral of Engineering in Machine Design. Public review: Kungliga Tekniska Högskolan, Room F3, Lindstedtsvägen 26, Stockholm, at 9:00 on November 22, 2013.

Printed in Sweden

Universitetsservice US-AB

Abstract

To attract more customers and compete with other modes of transportation, railway transport needs to ensure safety, punctuality, high comfort, and low cost; wheel–rail adhesion, i.e., the transmitted tangential force in the longitudinal direction during driving and braking, plays an important role in all these aspects. Adhesion needs to be kept at a certain level for railway operation and maintenance. However, wheel–rail contact is an open system contact. Different contaminants can present between the wheel and rail surfaces, forming a third-body layer that affects the adhesion. Prediction of wheel–rail adhesion is important for railway operations and research into vehicle dynamics; however, this prediction is difficult because of the presence of contaminants.

This thesis deals with wheel–rail adhesion from a tribological perspective. The five appended papers discuss wheel–rail adhesion in terms of dry conditions, lubricated conditions, leaf contamination, iron oxides, and environmental conditions. The research methodologies used are numerical modelling, scaled laboratory experiments, and field tests. The research objective is to understand the mechanisms of the adhesion loss phenomenon.

A numerical model was developed to predict wheel–rail adhesion based on real measured 3D surfaces. Computer simulation indicates that surface topography has a larger impact on lubricated than on dry contacts. Plastic deformation in asperities is found to be very important in the model. Ball-on-disc tests indicate that water can give an extremely low adhesion coefficient on smooth surfaces, possibly due to surface oxidation. Investigation of lubricated contacts at low speed indicates that oil reduces the adhesion coefficient by carrying a normal load, while adhesion loss due to water depends on the surface topography, water temperature, and surface oxidation. A field investigation indicates that leaves reduce the friction coefficient because of the chemical reaction between leaves and bulk materials. The thickness of the surface oxide layer was found to be an essential factor determining adhesion reduction. Pin-on-disc experiments found a transition in the friction coefficient with regard to the relative humidity, due to a trade-off between the water molecule film and the hematite on the surface.

Keywords: Adhesion; Wheel–rail contact; Contaminants; Tribology

Preface

The work in this thesis was carried out between September 2009 and September 2013 at the Department of Machine Design at Royal Institute of Technology (KTH), Stockholm, Sweden.

I would like to thank the SAMBA Swedish research program and especially KTH Railway Group, Trafikverket and SLL for funding this project. I would like to thank China Scholarship Council to provide me a four-year financial support. My main supervisor Prof. Ulf Olofsson deserves particular thanks for giving me the chance to do this work, guiding me into the field of tribology, discussing my research work from the beginning to the end and for his excellent supervise. Special thanks also to Dr. Anders Söderberg as my co-supervisor for discussions especially over my thesis. Besides, I would like to thank following people for contributing to my research work: Dr. S. Björklund, Prof. M. Berg, Dr. R. Enblom, Dr. S. Abbasi, Dr. E. Bergseth, Mr. P. Carlsson, Dr. R. Nilsson, Dr. H. Chen, Mr. U. Bik and all of my colleagues.

In addition, I want to gratefully acknowledge all my friends for being with me to combat long dark winter and have fun in the cool summer here.

Finally, I want to show my most heartfelt gratitude to my parents, for your supports and encouragements during my overseas study. Your efforts are beyond any words to be expressed!

Stockholm, September 2013

Yi Zhu

List of appended papers

This thesis consists of a summary and the following appended papers:

Paper A

Y. Zhu, U. Olofsson, A.Söderberg: "Adhesion modeling in the wheel-rail contact under dry and lubricated conditions using measured 3D surfaces".

Tribology International 61 (2013) 1-10.

The main part of the writing and adhesion modelling were performed by Zhu.

Paper B

Y. Zhu, U. Olofsson: "An adhesion model for wheel–rail contact at the micro level using measured 3d surfaces".

Accepted for publication in a special issue of *Wear*.

The model and the main part of the writing were performed by Zhu.

Paper C

Y. Zhu, U. Olofsson, K. Persson: "Investigation of factors influencing wheel–rail adhesion using a mini traction machine".

Wear 292-293 (2012) 218-231.

The experimental works and the main part of the writing were performed by Zhu.

Paper D

Y. Zhu, U. Olofsson, R. Nilsson: "A field test study of leaf contamination on the rail head surfaces".

IMechE Part F: J. of Rail and Rapid Transit. Available online, DOI: 10.1177/0954409712464860

The main part of the writing and evaluation were performed by Zhu.

Paper E

Y. Zhu, U. Olofsson, H. Chen: "Friction between wheel and rail: a pin-on-disc study of environmental conditions and iron oxides".

Tribology Letters. Available online, DOI: 10.1007/s11249-013-0220-0

The main part of the experiments, analysis and writing were performed by Zhu.

List of published papers not included in this thesis

R. Lewis, S. Lewis, **Y. Zhu**, S. Abbasi, U. Olofsson: "The Modification of a Slip Resistance Meter for Measurement of Railhead Adhesion".

IMechE Part F: J. Rail and Rapid Transit 227(2) 196–200, 2013.

S. Abbasi, U. Olofsson, **Y. Zhu**, U. Sellgren: "Pin-on-disc study of the effects of railway friction modifiers on airborne wear particles from wheel–rail contacts".

Tribology International 60 136-139, 2013.

U. Olofsson, **Y. Zhu**, S. Löfving, J. Casselgren, L. Mayer, R. Nilsson: "An optical sensor for the identification of low adhesion in the wheel rail contact".

International Journal of Railway Technology. Article in press.

U. Olofsson, **Y. Zhu**, S. Abbasi, R. Lewis, S. Lewis: "Tribology of the wheel–rail contact – aspects of wear, particle emission and adhesion".

Vehicle System Dynamics 51 (7) 1091-1120, 2013; Special Issue: State of the art papers of the 23rd IAVSD Symposium.

Contents

1	Introduction.....	1
1.1	Wheel–rail contact conditions	2
1.2	Adhesion, traction, and friction.....	4
1.3	Rough surfaces.....	8
1.4	Wheel–rail adhesion under contaminated conditions	10
1.5	Adhesion modelling	12
1.6	Measures to improve wheel–rail adhesion.....	14
1.7	Research questions	15
2	Summary of appended papers.....	16
3	Discussion.....	19
4	Conclusions	24
5	Future work.....	25
	Appendix I: A simplified model for calculating the required adhesion coefficient.....	26
	References	27

Appended papers

- A. Adhesion modeling in the wheel-rail contact under dry and lubricated conditions using measured 3D surfaces.
- B. An adhesion model for wheel–rail contact at the micro level using measured 3d surfaces.
- C. Investigation of factors influencing wheel–rail adhesion using a mini traction machine.
- D. A field test study of leaf contamination on the rail head surfaces.
- E. Friction between wheel and rail: a pin-on-disc study of environmental conditions and iron oxides.

1 Introduction

Railway transport is generally acknowledged for its low cost, environmental friendliness, energy efficiency, and fast speed (over short and medium distances) compared with other means of transportation. Of all the factors affecting railway operation, safety is the primary concern. For passengers and customers, accurate timetable, good ride comfort (for passengers), and low cost are also important. Therefore, railway operators and maintainers need to keep train service punctual, relatively quiet, comfortable, and low in cost to attract customers and compete with other means of transportation. Adhesion, the transmitted tangential force in the longitudinal direction between the railway wheel and rail, affects all the factors mentioned above. First, wheel–rail adhesion must be sufficient to fulfil safety and punctuality requirements. Generally, low adhesion during braking will extend the braking distance, which is a safety issue. Low adhesion during driving reduces the acceleration, leading to timetable disruption. Second, wheel–rail adhesion should be low to keep the energy consumption down. Furthermore, if the adhesion is too high, wheels and rails are subject to excessive shear stress, leading to severe wear and surface fatigue [1]. Third, the friction coefficient between the wheel and rail should not vary too much so as to avoid stick–slip oscillation, which may induce rail corrugation leading to noise and poor comfort [2]. Last, maintenance measures related to wheel–rail adhesion should be cost effective. As the wheel–rail contact is an open system, the adhesion between the wheel and rail is inevitably affected by contaminants. Contaminants, which refer to foreign substances applied both intentionally and unintentionally to the wheel–rail interface, can make wheel–rail adhesion either too high or too low and difficult to predict. The prediction of wheel–rail adhesion is important not only to railway operation but also to the simulation of multi-body vehicle dynamics. Dynamic modellers attempt to improve dynamic models by implementing key adhesion-related factors in a computationally fast contact model. Such relationships between key factors and wheel–rail adhesion are based on investigation of the adhesion loss phenomenon. However, the mechanisms of this phenomenon are not yet well understood. This thesis examines the adhesion between railway wheels and rails from a tribological perspective. The aim of the research is to understand the mechanisms of the adhesion loss phenomenon. Papers **A** and **B** investigate the wheel–rail adhesion under dry and lubricated conditions using numerical simulations. Papers **C** and **E** provide experimental methods for scaled laboratory tests to examine the influence of lubricants and environmental conditions on the adhesion and friction. Paper **D** reports a full-scale field test with a focus on leaf contamination on rails.

This chapter presents the research background and motivation as well as a literature review. Section 1.1 provides some basic information on contact conditions between the wheel and rail. Section 1.2 defines adhesion, traction, and friction and discusses some measurement techniques. The surface topography and surface roughness of wheels and rails are discussed in Section 1.3. Section 1.4 presents the requirements for wheel–rail adhesion and an overview of relevant contaminants. Adhesion modelling is reviewed in

Section 1.5, while Section 1.6 briefly discusses certain measures that can improve adhesion. Finally, the research questions are presented in Section 1.7.

1.1 Wheel–rail contact conditions

Since adhesion is a force acting at the wheel–rail interface, wheel–rail contact conditions need to be discussed first. Unlike some other means of transportation, such as road vehicles and aircraft, railway vehicles run on rails that are fixed to the ground through sleepers and ballasts or slabs. The guiding performance of the railway vehicle system is determined by interaction between the wheel and the rail profiles, which refer to the shapes of the wheel and rail [3]. Figure 1.1 shows a schematic of a new railway wheel and a new rail. A typical railway wheel has a wheel tread, where the wheel is usually in contact with the rail, and a flange to improve the lateral guiding. Wheel profiles are conical (shown as “a” in Figure 1.1) to facilitate steering performance. Rails are mounted with an inwards inclination (shown as “b” in Figure 1.1) to match the conical wheel profile and for better load transfer to the sleepers and ballasts. Depending on the wheel and rail profiles, the curvature of the track, and the wheel position, the exact contact position can be determined [1]. In most cases, the contact positions between the wheel and the rail are wheel tread–rail head contact and wheel flange–rail gauge contact. These two basic contact positions are shown in Figure 1.1 as “c” and “d”. Along straight tracks, the wheel tread and rail head are likely to be in contact, while wheel flange–rail gauge contact occurs along curved tracks. Adhesion research considers only the wheel tread–rail head contact.

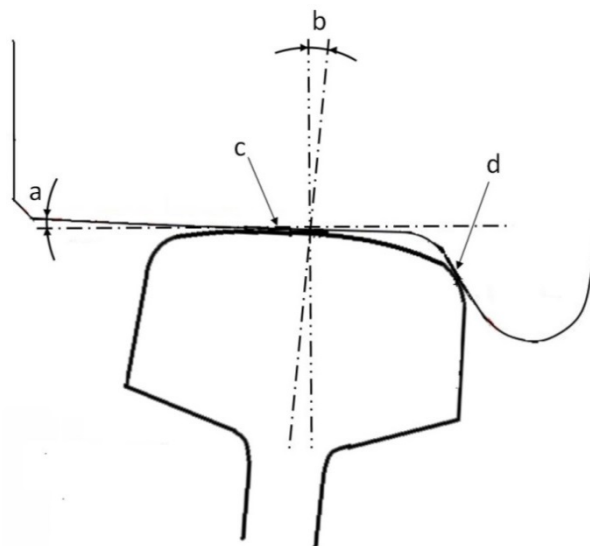


Figure 1.1. Schematic of wheel–rail contact positions [4]: a) conical wheel profile; b) rail inclination; c) wheel tread–railhead contact; and d) wheel flange–rail gauge contact.

Contact conditions, such as contact pressure and contact area, depend greatly on the material properties. Railway wheels and rails are often made of steel. Table 1.1 shows the material compositions of a widely used UIC 900A rail and an R7 wheel. UIC 900A rail material is reported to have a hardness of 300 HB and a minimum tensile strength of 863 N/mm² [5]. R7 wheel material is a little softer, in the hardness range of 229–277 HB,

with tensile strength in the range of 730–890 N/mm² [6]. However, the hardness can vary depending on the measurement position, traffic density, time in service, curve radius, and lubrication [7]. Other types of wheel and rail steel differ somewhat in material composition and hardness, as discussed elsewhere [1,8,9]. Since both wheel and rail materials are hard, the contact area between the wheel and rail is comparatively small, typically 1 cm² in size [1]. The size of the contact area varies depending on the contact position and geometry of the contact bodies. On the other hand, railway vehicles are often very heavy for safety and robustness, so the small contact area needs to transfer a very high axle load, causing very high contact pressure.

Table 1.1. Material composition comparison [8].

Chemical composition (wt %)	C	Si	Mn	P	Ni	Cr
UIC 900A rail	0.6–0.8	0.15–0.5	0.8–1.3			
R7 wheel	0.52	0.4	0.8	0.035	0.3	0.3

Lewis and Olofsson [8] examined the contact conditions in the two types of contacts, as shown in Figure 1.2. In the contact between the wheel tread and the rail head, both contact pressure and sliding speed are lower than in the contact between the wheel flange and the rail gauge. Severe contact conditions will cause more wear, so the wheel flange–rail gauge contact is usually intentionally lubricated. Consequently, the measured friction coefficient is usually lower on the rail gauge, where it is lubricated, than on the rail head [7]. This thesis examines the contact between the wheel tread and rail head.

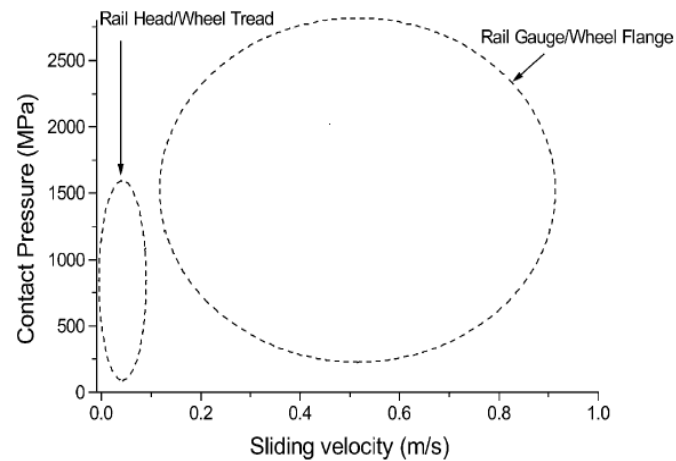


Figure 1.2. Contact conditions in the wheel–rail contact [8].

Contact pressure between the railway wheel and rail can be determined experimentally. Marshall et al. [10] used ultrasound to quantify the stress distribution between statically loaded wheel and rail specimens. The experimental results were compared with those of a numerical model based on boundary element methods proposed by Björklund and Andersson [11]. Some new techniques, such as using pressure-sensitive paper on a short section of the rail surfaces, as presented by Lin et al. [12], can measure the contact pressure between the wheel and rail. Embedded fibre bragg grating sensors [13] have some potential for measuring wheel–rail contact area and contact pressure. However,

since the contact position and contact area between the railway wheel and rail vary constantly, measuring contact conditions is difficult; the main approach to assessing the contact area and contact pressure is consequently based on calculation. The calculations can be conducted using Hertzian theory assuming an infinite half space. The CONTACT software package [14], based on the boundary element method, is widely used in the railway research community and is regarded as a complete solution. A similar method for calculating contact pressure between rough surfaces has been proposed by Björklund and Andersson [11]. A finite-element model has been developed by Telliskivi and Olofsson [15], who compared their model with Hertzian methods and CONTACT. They pointed out that the half-space assumption and material model could greatly influence the contact area and pressure in the wheel flange–rail gauge contact. In the contact between the wheel tread and rail head, the half-space assumption is valid, so methods based on Björklund and Andersson [11] are used here.

1.2 Adhesion, traction, and friction

From a strict tribological point of view, adhesion is the force required to separate two surfaces that have been brought into contact, and is usually used to describe how well surface coatings or paints are bonded to the surfaces they coat [16,17]. However, the term “adhesion” has become widely used in the wheel–rail research community to refer to the tangential force exerted in the wheel–rail contact, for example, as used by Fletcher et al. [18] and Lewis [19]. Friction force is defined as the resistance encountered by one body moving over another [1].

The difference between adhesion and friction is illustrated in Figure 1.3. Figure 1.3 a) shows a block sliding at velocity, v , along a stationary plane. The block is subject to a normal force, F_N , attributable to the mass of the block, m , and a horizontal pull, F . The horizontal force that opposes the motion of the block is deemed the friction force, F_f . The static friction force is defined as the horizontal force required to initiate sliding, while the kinetic friction force is the horizontal force required to maintain sliding [1]. Generally, the static friction is higher than the kinetic friction. The ratio between the friction force and the normal force is referred to as the friction coefficient:

$$\mu_f = \frac{F_f}{F_N} \quad (1.1)$$

Figure 1.3 a) presents a case of pure sliding, and the friction force in a dry contact depends on asperity ploughing (abrasion) and atomic interaction (adhesion). Ploughing is due to the interaction of surface asperities during sliding. In addition, hard particles and wear debris may also contribute to ploughing. The adhesion force arises from the attractive force between asperity contacts [20]. For most metal pairs, the coefficient of friction from the ploughing component is 0–1.0, while that from the adhesion component is 0–0.4 [21].

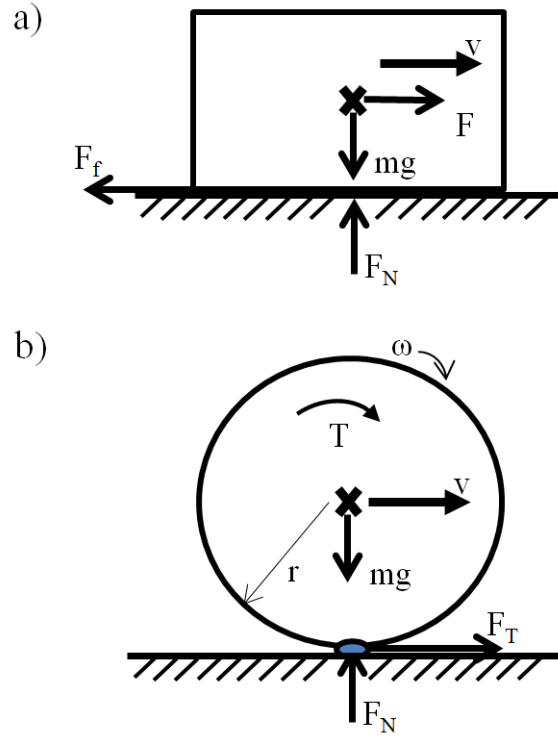


Figure 1.3. Schematic of a) a pure sliding contact and b) a rolling–sliding contact under acceleration (X is the gravity centre; all forces in the figure are acting on either the block or the wheel).

Figure 1.3 b) shows a cylinder rolling along a stationary plane surface. This is analogous to the case of a wheel rolling along a rail. The wheel is subject to normal force, F_N , and travels along the rail at velocity v . The wheel is subject to torque, T , which maintains the angular velocity of the wheel, ω , and also causes a reactive tangential force, F_T , at the wheel–rail interface. The tangential force of a driving wheel is known as traction, which ultimately propels the wheel along the rail. During deceleration, the tangential force, F_T , opposes the running direction due to the braking torque, T , applied anticlockwise. The tangential force in the longitudinal direction during both acceleration and deceleration is referred to as adhesion. The ratio between the adhesion force and the normal force is known as the adhesion coefficient [4]:

$$\mu_a = \frac{F_T}{F_N} \quad (1.2)$$

The adhesion and traction mentioned above refer to the transmitted tangential force which wheels actually have, while the tractive force refers to the applied force.

During acceleration or when overcoming losses while driving at constant speed, the tangential velocity at the wheel surface, ωr , of a driven wheel will always be greater than its body velocity, v . The difference between the tangential velocity of the wheel, ωr , and the body velocity, v , divided by the rolling velocity is referred to as creep or creepage and is usually given as a percentage [22]:

$$\xi = \frac{v - \omega r}{\frac{1}{2}(v + \omega r)} \times 100\% \quad (1.3)$$

Since adhesion is the tangential force in the longitudinal direction, the creep discussed here refers to longitudinal creep and the contact refers to the wheel tread–rail head contact. Sometimes the wheel’s body velocity, v , is also used as the denominator of Equation (1.3) in railway dynamics assuming the creep is small ($v \approx \omega r$). In the railway literature, slip is sometimes used instead of creep. However, to distinguish slip from micro slip, the term “creep” will be used throughout this thesis instead of “slip”.

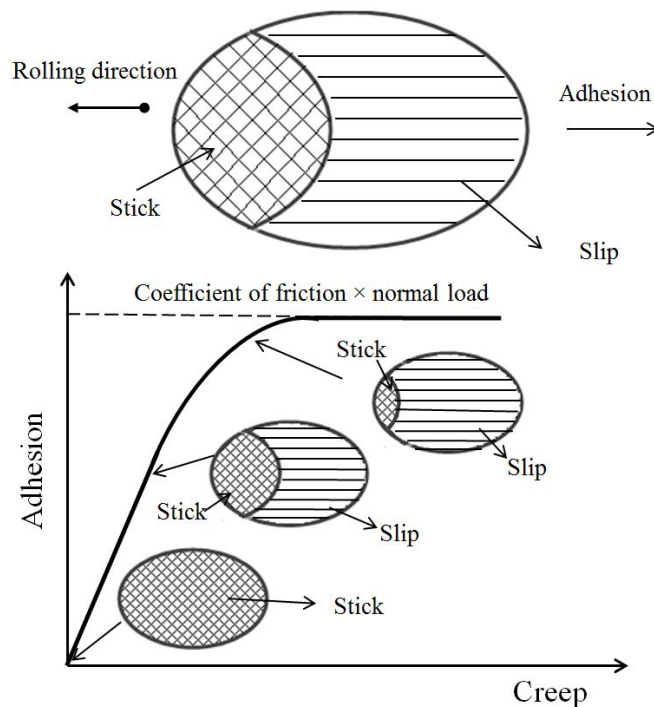


Figure 1.4. A creep curve showing the relationship between adhesion and creep.

Figure 1.4 shows the relationship between creep and adhesion for a typical dry wheel–rail contact. This plot of adhesion versus creep is known as the creep curve. When the creep is zero, the whole contact area sticks and no tangential force is transmitted, in what is known as “free rolling”. However, zero creep does not exist in reality, since the inevitable deformation between two contact bodies results in a certain amount of creep. Slip occurs at the trailing edge and spreads forward through to the contact area as the adhesion increases. The slip region increases and the stick region decreases resulting in a rolling–sliding contact until pure sliding appears. In that state, the adhesion equals the friction force between two bodies under pure sliding conditions. When the creep is small, the adhesion increases in an approximately linear fashion with increased creep. After that, the slope of the creep curve (the increasing rate of adhesion) decreases with increased creep. At approximately 1–2% creep, the slope of the creep curve and the stick region are extremely small, and the adhesion is very close to the friction. For a typical creep curve in the railway context, the adhesion decreases after reaching its maximum [23], typically at 1–2% creep under dry and clean conditions. The adhesion at that point is considered the maximum tangential force that approximately equals the friction force.

In reality, because part of the friction is utilized by the lateral and spin forces, and also because the load is not equally distributed between all axles and wheels, the maximum

adhesion (or limiting friction) in the longitudinal direction is less than the total friction [24]. Therefore, most adhesion research, which assumes that friction is used only for adhesion, overestimates the resulting adhesion. The adhesion and friction coefficients are schematically depicted in Figure 1.5. The friction coefficient is larger than the adhesion coefficient under both clean and contaminated conditions, although the values under clean conditions are larger than those under contaminated conditions. Note that the friction coefficient shown in the figure is kept constant to enable comparison between the friction and adhesion coefficients; in reality, the coefficient of friction is not constant.

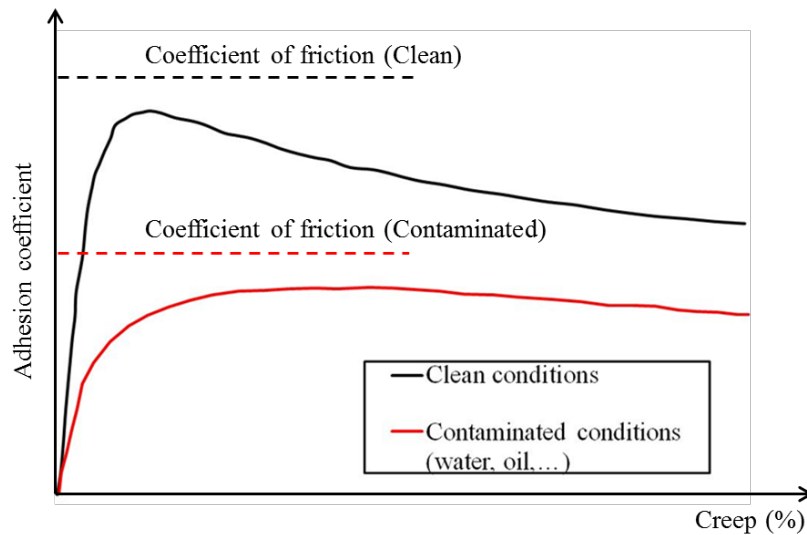


Figure 1.5. Schematic of the adhesion curve and coefficient of friction under clean and contaminated conditions. The solid lines indicate the adhesion coefficient while the dashed lines indicate the coefficient of friction (modified from Polach [23]).

The adhesion between the wheel and rail can hardly be measured directly, although friction can be measured on the rail surface. The most accurate way of measuring wheel–rail adhesion is to use instrumented trains that measure the adhesion between the actual railway wheel and the rail. However, making measurements using an instrumented train is expensive, complicated, and insufficiently controllable. Other measurement devices include a hand-pushed tribometer and a vehicle companion Tribo-Railer [25]. Both of these devices use small steel wheels rolling on the rail, though based on different principles. The wheel is connected to a clutch that is gradually engaged; at a certain point, the torque on the wheel overcomes the friction between the wheel and rail, causing the wheel to slip. It must be noted, however, that this measurement is of the friction between the device being used and the rail, not between the actual wheel and rail, and hence can only be used as an indication of the maximum adhesion available. Moreover, the results obtained using these two measurement devices may differ slightly even when used under similar conditions. For example, a hand-pushed tribometer and a Tribo-Railer give different friction coefficient values when both are used to make measurements on dry railhead [25] because of the differences in measuring speed, measuring length, wheel size, and operating principles.

A new device called the pendulum rig [26] (shown in Figure 1.6) has recently been investigated. Based on the energy loss principle, as used in the Charpy impact test, the device is able to measure the friction coefficient between the rubber pad and the rail head over a very short section (i.e., 12.7 cm) of rail. Regarding the measuring length, a pendulum rig is more suitable for investigating areas of adhesion loss on the rail head, which are often very localized, such as short sections contaminated with oil, grease, and leaves, than are the measuring devices mentioned above. In addition, the pendulum rig can also be used on a piece of rail section in the laboratory.

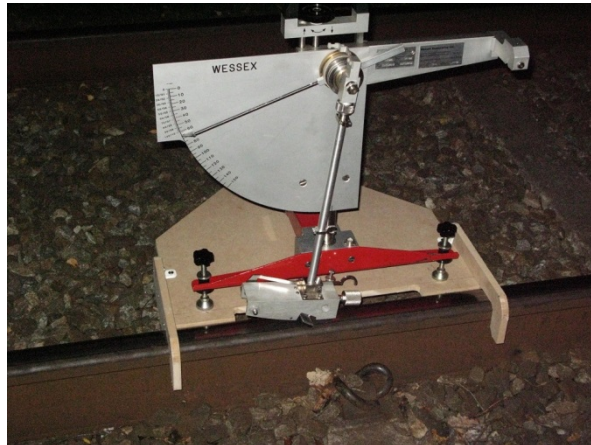


Figure 1.6. A field measurement being made using the pendulum rig.

1.3 Rough surfaces

In tribology, the science and engineering of interacting surfaces in relative motion, it is crucial to investigate what the surfaces look like on a small scale. All engineered surfaces are somewhat rough, even when the most advanced surface finishing techniques are used. In most machine elements, surface topography affects friction, wear, and longevity. In dry contacts, surface topography significantly affects the contact area; for example, as illustrated in Figure 1.7, the real contact area is much smaller than the nominal contact area [27]. In lubricated contacts, the surface topography is important for film formation, particularly in elasto-hydrodynamic lubrication (EHL) [28].

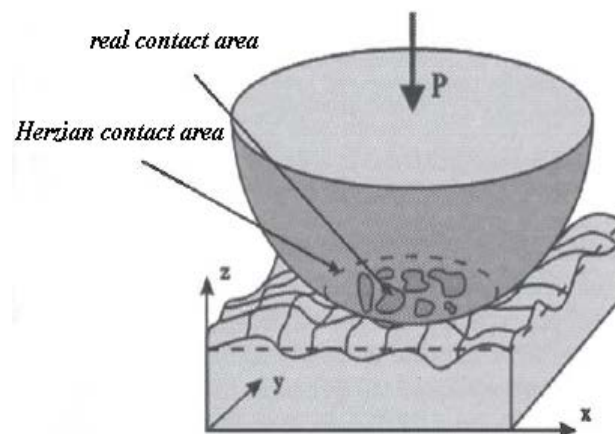


Figure 1.7. Schematic of contact between rough and smooth surfaces [27].

To investigate the adhesion and friction between wheels and rails, the surface roughness or surface topographies of wheels and rails need to be considered. Wheels and rails are finished by grinding and turning, respectively. Though the newly finished surfaces of wheels and rails must meet national standards, the initial surface topographies are usually run-in very quickly. Lundmark et al. [29] investigated the influence of traffic on both surface roughness and rail profile after grinding or re-turning of wheels by measuring their surface roughness on heavy-haul lines. They found that the S_a (i.e., arithmetical mean height of the surface) value of the newly ground rail surface changed from $\sim 10 \mu\text{m}$ to $\sim 1 \mu\text{m}$ after the first 1.5 days of traffic. However, 2D roughness, R_a , is usually used for rails. The R_a value of newly ground rail surfaces must not exceed $10 \mu\text{m}$, according to the Swedish National Traffic Administration. The 2D and 3D roughness parameters are discussed by Thomas [30]. Wheel and rail profiles are often measured in situ using the MINIPROF system [31], while surface topography can be measured using, for example, a stylus instrument or atomic force microscope. However, these techniques require the use of cut-out wheel/rail sections, making them unsuitable for field measurements. In addition, the replica technique is often used to “copy” real surfaces in the field to create negative images; surface replicas can then be measured using a stylus instrument [7] or an optical surface profiler [29].

Figure 1.8 shows two types of real measured surfaces cut from actual wheels and rails: unused (low-roughness) and sand-damaged (high-roughness) pairs (for more details on the surfaces, see Marshall et al. [10]). These two pairs of surfaces are used in a numerical simulation in this thesis. A Form Talysurf PGI 800 stylus device (Taylor Hobson) with a resolution of 3.2 nm was used to measure the surface topographies of wheels and rails. The unused or low-roughness pair had R_a values of 4.11 and $2.65 \mu\text{m}$ for the wheel and rail, respectively; this roughness is typical of unused surfaces [29]. The sand-damaged or high-roughness pair had R_a values of 12.45 and $20.38 \mu\text{m}$ for the wheel and rail, respectively; this roughness is fairly high but still can be found in the field [32]. Arias-Cuevas et al. [33] also reported that the sand used as a friction modifier in the Netherlands can produce an R_a value of over $20 \mu\text{m}$ on surfaces with only 1% slip.

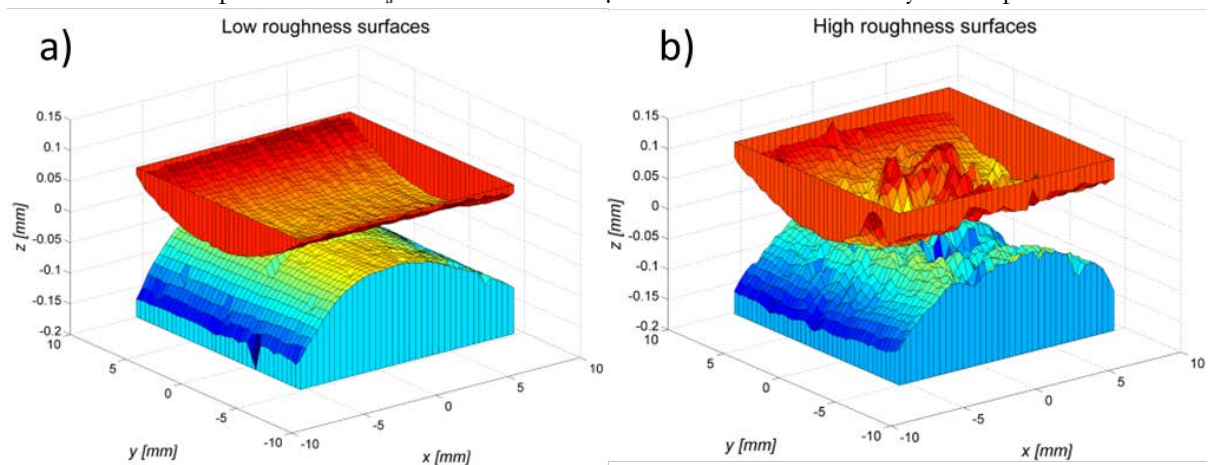


Figure 1.8. Measured 3D wheel and rail surfaces: a) low-roughness pair (unused); b) high-roughness pair (sand-damaged); the surfaces were cut and first used by Marshall et al. [10].

1.4 Wheel–rail adhesion under contaminated conditions

Adhesion coefficient requirements can be divided into three categories: those needed for 1) driving or braking the rolling stock at a given full capacity, 2) adhering to the timetable, and 3) ensuring safety [34]. Figure 1.9 schematically shows the required adhesion coefficients according to these three categories. It should also be noted that the adhesion coefficient requirements also depend on the type of rolling stock, traction and braking systems, number of powered/braking axles, etc. [34]. For example, a metro vehicle or a commuter train usually requires relatively high acceleration and deceleration due to the short intervals between stops [24]. An acceleration of 1.5 m/s^2 measured in a metro vehicle [35] requires an adhesion coefficient of at least 0.15. A simplified model that can explain the relationship between acceleration/deceleration and the adhesion coefficient/friction coefficient is presented in Appendix 1. In this thesis, a commuter train is used as the object of the computer simulation and a metro line is used in investigating leaf contamination.

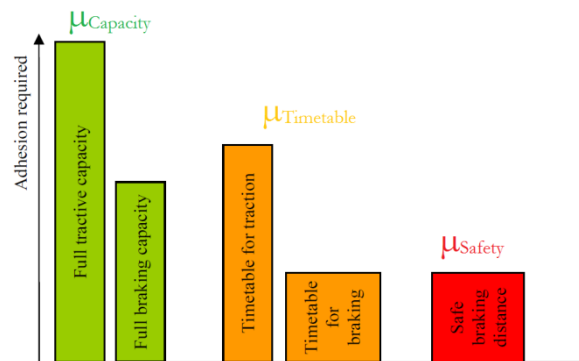


Figure 1.9. Common adhesion requirements in railway transportation [34]; the bar height is proportional to the maximum required adhesion coefficient in the Netherlands.

On the other hand, the adhesion coefficient is limited by the coefficient of friction between the wheel and rail despite other factors such as dynamic load variation [24]. For the steel–steel contact under dry, clean conditions, the coefficient of friction is approximately 0.6, which obviously fulfils all adhesion requirements. However, the wheel–rail interface is an open system, meaning that contaminants can enter the contact and affect the friction levels, making the wheel–rail adhesion too high or too low. Table 1.2 shows the friction coefficient measured under different conditions [1]. The friction coefficients under some conditions shown in the table are below 0.1, meaning that the actual adhesion coefficients are even lower and can hardly achieve the level required for safety [4].

Table 1.2. Friction coefficients measured on metro lines using a hand-pushed tribometer [1].

Conditions	Temperature (°C)	Friction coefficient
Sunshine, dry rail	19	0.6–0.7
Recent rain on rail	5	0.2–0.3
A lot of grease on rail	8	0.05–0.1
Damp leaf film on rail	8	0.05–0.1

Since the wheel–rail system is an open system, any contaminants present between the wheel and rail affect the adhesion. Contaminants such as water, iron oxide, and leaves, which are unintentionally present on the rail [1] (“natural third-body materials”), should be distinguished from flange lubricants and friction modifiers deliberately applied to the rail or wheel (“artificial third-body materials”). All of the above can be termed “third-body materials” [36] that form a third body between the bulk materials of the wheel and rail. Third bodies, such as iron oxide or leaves, sometimes become chemically bonded to the surfaces of the bulk materials. Therefore, in practice, the actual materials forming the wheel–rail contact can differ chemically from the wheel and rail steels forming the actual wheel and rail, as shown in Figure 1.10.

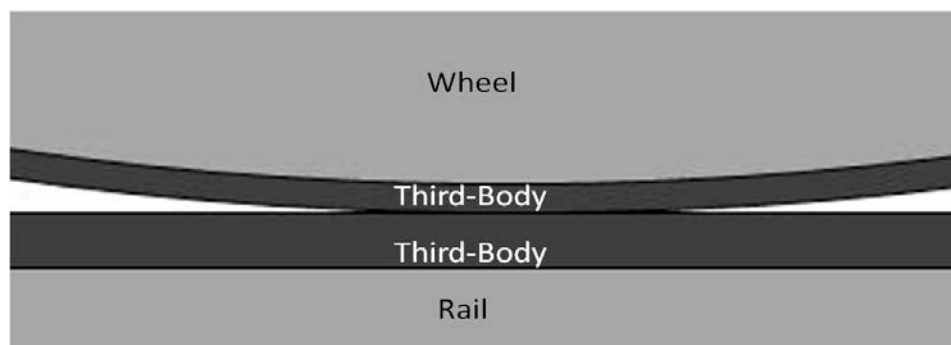


Figure 1.10. The third-body layer between the bulk materials in the wheel–rail contact [1].

Water and oil can be found on rails and wheels, and both of them can reduce the adhesion coefficient if entrained into the contact. Neither water nor oil is intentionally applied to the wheel–rail interface. Water usually originates from precipitation, which is unavoidable, while oil is intentionally applied to the gauge to reduce flange wear but is usually squeezed onto the rail head or is present on the rail head due to incorrect application. Water and oil are called “lubricants” (from a tribological perspective) in this thesis for convenience. Full-scale test rig [37] and field testing [38] results indicate that the adhesion coefficient declines significantly with increasing rolling speed under wet conditions, while the adhesion coefficient changes little with speed but remains low under oil-lubricated conditions. Chen et al. [39] found that the surface roughness, surface orientation, and water temperature greatly affected the adhesion coefficient measured in a twin-disc rolling contact machine. The effects of oil and water mixtures were studied using a twin-disc test rig [40] and a wheel–rail simulation facility [41]; both these studies found that it is the oil in the mixture that has the dominant effect in reducing adhesion/friction. This thesis also investigates the adhesion reduction by comparing the effects of water with those of oil, since both these substances can be considered lubricants from a tribological point of view.

Using small-scale test rigs, Beagley et al. [42–44] studied wheel–rail adhesion taking water, oil, and wear debris into account. They found that a small amount of water mixed with substantial quantities of debris could form a paste that significantly reduced the adhesion; however, the paste was squeezed aside if the amount of water was sufficient. When oil is present, the adhesion coefficient depends on the quantity of oil. Above a certain amount, the adhesion coefficient has been found to be constant depending on the

characteristics of the particular oil used. Nakahara et al. [45] found that various oxides formed under wet conditions, while Suzumura et al. [2] and Ohno and Ogawa [46] found that oxide layers significantly influenced the adhesion coefficient. Olofsson and Sundvall [47] and Hayashi et al. [48] pointed out that temperature and humidity greatly affected the adhesion coefficient between the wheel and rail. It is therefore essential to take iron oxides into account when the examined contact is dry or wet. However, little research has investigated the influence of environmental conditions on the coefficient of friction by comprehensively examining iron oxides, since the oxidation process is transient, making it difficult to study.

Rail services worldwide have been disturbed by crushed leaf layers on the rail head, which can reduce the friction coefficient to below 0.1 [49]. According to Fulford [50], leaves do not have to fall precisely on the tracks, as even leaves that have fallen beside the line can be stirred up by the turbulence of passing trains and happen to land on the rail surface. The leaves are then crushed by passing wheels to form a tarnished layer that is chemically bonded to the railhead (see photo in Figure 1.11). The costs associated with low adhesion, to which leaves are thought to make a major contribution, can be very high [51,52]. Leaf fall can also considerably disturb traffic on the network [34]. Research into leaf contamination and low adhesion has used various methods, including actual trains [53] as well as pin-on-disc [47,54], twin-disc [55,56], and ball-on-disc [57] test rigs. The results indicate that while crushed leaves alone can reduce the friction coefficient, the friction coefficient decreases even more in the presence of water or high humidity. Adhesion problems have even been reported on tracks displaying no visible signs of a crushed leaf layer [54]. As the mechanism of the low adhesion caused by leaves is not understood, research investigating the actual tarnished layer found on tracks would help us understand this low-adhesion phenomenon.

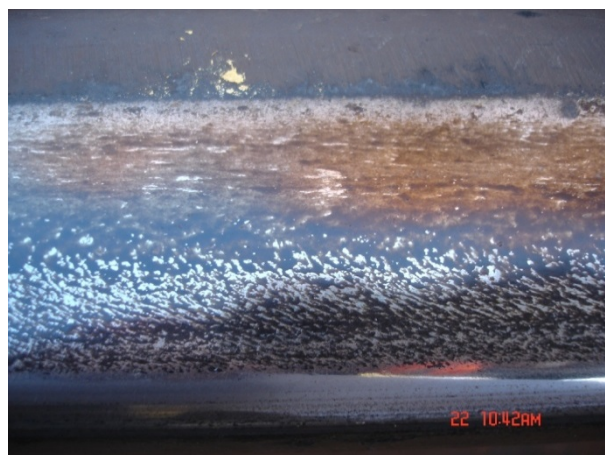


Figure 1.11. A tarnished layer on the railhead surface caused by leaves (source: R. Nilsson).

1.5 Adhesion modelling

Although wheel–rail adhesion can be measured in the field to some extent, doing so is expensive, complicated, and insufficiently controllable. High-accuracy predictions of wheel–rail adhesion by computer would produce considerable cost savings. Modelling

rolling contacts is one of the most important and fundamental parts of adhesion modelling. Widely used contact models, such as CONTACT [14] and FASTSIM, were developed under the assumption of rolling contact with dry friction; they are accordingly valid for and mainly used to investigate the wheel–rail contact under dry and uncontaminated conditions. These software packages are based on certain simplifications, such as the infinite half space. Chen et al. developed 2D and 3D numerical adhesion models [58,59] to study wheel–rail adhesion under water-lubricated conditions. The 3D model [59] considers both the water temperature and surface roughness orientation. These models simulate wheel–rail adhesion in a stationary state and assume a constant asperity friction. Tomberger et al. [60] recently presented an adhesion model comprising micro contact, water lubrication, and flash temperature and introduced a simple temperature-dependent local friction coefficient model. However, in lubricated contacts, the boundary friction coefficient (i.e., the maximum friction coefficient in a Stribeck curve when the speed is close to zero) is difficult to determine and is usually obtained experimentally. In dry contacts, the friction coefficient between asperities is difficult to determine as we lack a physical model. Plasticity is another essential factor that significantly changes the contact pressure and area but is also difficult to take into account. Moreover, other factors are coupled: for example, the flash temperature depends on the pressure distribution, which in turn depends on material properties closely related to the flash temperature. It is important to consider all these factors as well as their interdependence. Regarding lubricated contacts, most relevant studies of the wheel–rail contact consider only water-lubricated contacts. A possible extension would be to consider oil as well; this would allow comparisons that would help explain the different adhesion loss behaviours attributable to the two fluids. In addition, surface topography is often taken into consideration by using statistical methods to create surfaces [59,60]. However, statistical methods tend to create surfaces based on only certain parameters, such as surface roughness. These methods are convenient, as surface roughness can be varied in the numerical simulation, but the resulting surface topographies may differ greatly from real surface topographies found in the field. It would therefore be interesting to model wheel–rail adhesion using real measured wheel and rail surfaces; this would foster deeper insight into the influence of surface topography.

Another way of modelling adhesion is to combine a fast contact model with some measurement results. Polach [23] presents an extended method for simulations involving large creep at the adhesion limit. The required additional parameters are based on measurements made on locomotives. This solution provides better agreement with measurements at high traction creep than do other methods used in simulating multi-body vehicle dynamics. Zhang et al. [37] made measurements using a full-scale roller rig and applied a modified FASTSIM model to achieve better agreement with measurements. The latest work by Meierhofer et al. [61] developed a third-body model that comprises oxide layers and wear debris. The third-body model was based on the results of twin-disc testing. Before we can fully understand the characteristics of wheel–rail adhesion and develop a physical model, it would be practical to model wheel–rail

adhesion with the help of experimental results. The drawback of this method is that the model developed will be valid only under particular assumptions, because the model is based on experimental results obtained under specific conditions.

1.6 Measures to improve wheel–rail adhesion

Wheel–rail adhesion can be improved by slip control and by modifying the friction level between the wheel and rail. Depending on the requirements, a targeted adhesion coefficient can be achieved by controlling the slip. If the coefficient of friction between the wheel and rail barely attains or is even below the required adhesion coefficient, the slip should be very accurately controlled to achieve the maximum adhesion coefficient, which is the saturation point shown in Figure 1.5 [24]. This thesis mainly discusses how to modify the friction between the wheel and rail in order to improve the adhesion.

Friction management can be used to keep the friction coefficient between the wheel and rail within a desirable range. The ideal friction coefficient for heavy-haul traffic is shown in Figure 1.12. Friction modifiers can be applied to the wheel–rail interface to achieve a target friction coefficient. According to Kalousek and Magel [62], these modifiers are of three types:

- low-coefficient friction modifier (LCF)/lubricant in the wheel flange–rail gauge contact,
- high-positive friction modifier (HPF) in the wheel tread–rail head contact, and
- very-high-positive friction modifier (VHPF) for locomotives.

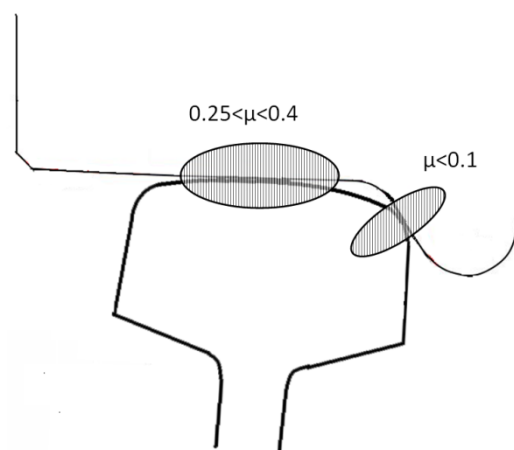


Figure 1.12. Ideal friction coefficients in the wheel–rail contact for heavy-haul traffic [62].

LCF can take the form of solids, oils, or greases usually applied to the high rail during curving to reduce the friction coefficient and wear. HPF is applied mainly to reduce short-pitch corrugation and squeal by introducing a positive slope after the saturation point on the creep curve [63] in order to avoid stick–slip oscillations. VHPF is used to restore adhesion under adhesion loss conditions. Due to its effectiveness and easy application, sand is the main VHPF used worldwide. Arias-Cuevas et al. [33,53] compared four types of sands differing in grain size using a combination of laboratory

(twin-disc) and field testing. Both test methods indicated that the adhesion improvement strongly depended on the sand particle size.

In addition to sand, other measures are taken to combat leaf contamination on rail surfaces, such as high-pressure water jetting, high-powered laser [54], and a magnetic track brake [64]. However, as leaf contamination on the rail is very localized and the contaminated depth varies, it is difficult to know how much material to remove from the rail head in each affected section in order to recover friction. Rail grinding is usually undertaken to control wear and fatigue, and to remove rail corrugations [1]. It can also be used on some track sections to remove contaminated layers chemically bonded to the rail material; however, the cost is high and the volume of material to be removed must be known in advance.

To improve these measures, it is important to discover the mechanism of the adhesion loss phenomenon. For example, research into water and wear debris found that a small quantity of water and debris can form a paste which can cause a significant adhesion reduction. The finding indicated that heavy rains can improve adhesion compared with that found under high humid conditions [42]. This thesis investigates leaf contamination to formulate suggestions regarding how much of the material needs to be removed by grinding in order to recover adhesion.

1.7 Research questions

The objective of this thesis is to understand the mechanisms of adhesion loss between the wheel and rail, investigating this matter from a tribological perspective. The following research questions can be derived from the objective:

- Is it possible to develop a numerical model with which to study the influence of factors such as speed, surface topography, temperature, and plasticity on the wheel–rail adhesion?
- Is it possible to experimentally simulate the lubricated wheel–rail contact in the laboratory environment; if so, how do experiments compare with the real situation?
- What is the mechanism of adhesion loss due to water and oil?
- How do leaves on rails reduce the friction coefficient? What is the key factor in this issue?
- How do environmental conditions and iron oxides influence the friction and adhesion?

2 Summary of appended papers

This thesis comprises five papers (papers **A** to **E**) that deal with wheel–rail adhesion both numerically and experimentally. Papers **A** to **C** discuss the characteristics of adhesion under dry and lubricated conditions, while paper **D** focuses mainly on leaf contamination on the rail. Paper **E**, which can be considered a further study of the previous work, looks closely at the influence of the presence of oxygen on the friction coefficient. The following are summaries of these five papers.

Using real measured surface topography, paper **A** attempts to develop a numerical model that can predict wheel–rail adhesion. The paper also investigates various factors influencing wheel–rail adhesion, mainly under water- and oil-lubricated conditions. The model comprises three parts: a normally loaded contact model, a rolling–sliding contact model, and a lubrication model. The model is based on the boundary element method presented by Björklund and Andersson [11] with the assumption of an infinite half space. In the normally loaded contact model, the effect of plastic deformation in asperities is simplified by introducing a constant allowable pressure. The rolling–sliding contact model assumes a stationary state that neglects time-dependent terms. In the lubrication model, water is assumed to be an incompressible fluid, while oil is assumed to be a compressible non-Newtonian fluid. The isothermal Reynolds equation is solved using finite difference methods. Results indicate that the inclusion of plastic deformation significantly changes the contact area, particularly for high surface roughness. With increased velocity, the adhesion coefficient decreases for both water- and oil- lubricated contacts, though the reduction differs greatly due to the different viscosities. Surface topography is important in lubricated contacts, and smooth surfaces reduce the adhesion coefficient more than do rough surfaces due to a large fluid load capacity (i.e., the normal load carried by fluids in percentage). The results are found to be in line with those obtained using statistical or experimental methods.

In paper **A**, the friction coefficient, which is obtained experimentally, is directly implemented in the model. However, the experimental results depend greatly on the testing conditions, which may differ from the numerical conditions. On the other hand, contact temperature is another important issue, especially in dry contacts at high speed and with large creep. Moreover, material properties that greatly affect the contact conditions can vary due to the contact temperature. Paper **B** focuses on dry conditions by further developing a local friction coefficient model and a contact temperature model. The model presented in paper **B** consists of a normally loaded contact model, a rolling–sliding contact model, a contact temperature model, and a local friction coefficient model. The sub-models presented in the two papers are shown in Figure 2.1. The local friction coefficient model is based on the Popov et al. [65] model, which calculates the local friction coefficient based on material properties and loading parameters. The contact temperature model is based on the work of Knothe and Liebelt [66], but we have extended it to the 3D situation. Plasticity is still dealt with via the allowable pressure, though the local allowable pressure now depends on the local contact temperature. The surfaces used in paper **B** are the same as those in paper **A**. However, surface topography

has a much smaller effect on the adhesion coefficient in dry rather than lubricated contacts; instead, surface topography affects parameters at the local level, such as contact pressure and contact temperature.

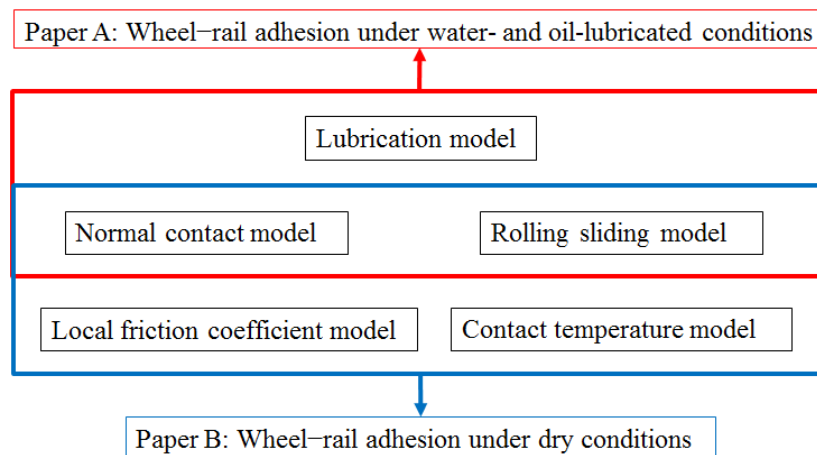


Figure 2.1. Sub-models presented in Papers A and B.

Scaled laboratory experimentation, another way to simulate real wheel–rail contact, can be compared with computer simulation. Full-scale tests and field measurements are more expensive and less controllable than are scaled experiments performed in a laboratory environment. Paper **C** investigates wheel–rail adhesion under water- and oil-lubricated conditions using a mini-traction machine (MTM). The MTM test rig consists of a steel ball and a steel disc, both of which can be rotated independently by two motors to generate a rolling–sliding contact. MTM test results are compared with real wheel–rail contact based on the calculated specific film thickness (Λ value). Experiments were conducted to test the traction curve (at constant speed) and the Stribeck curve (at constant slide-roll-ratio). A Form Talysurf PGI 800 stylus device (Taylor Hobson) was used to measure the surface topography on discs in 2D and 3D. A very-high-resolution atomic force microscope was used to examine small surface scratches in detail. The results indicate that surface topography has a greater influence on water-lubricated than oil-lubricated tests. Increased water temperature tends to increase the adhesion coefficient on rough surfaces, while the oil temperature has no significant affect. Smooth discs display a lower adhesion coefficient and fewer surface scratches in water tests than in oil tests.

Regarding leaf contamination, the main mechanism of the low friction is not known. Paper **D** presents a study of leaf contamination on the railhead surface that used real rail samples cut in the field. The friction coefficient on the railhead was measured in the field on five occasions over a year, and samples of the railhead were taken on each occasion. Electron spectroscopy for chemical analysis (ESCA) was used to determine the weight percent of all elements in the top 10 nm of the surface. Glow discharge optical emission spectrometry (GD-OES) was performed to analyse the elemental depth profile from a few nanometres to a depth of approximately 100 μm in the surface. The hardness of the contaminated layer was measured using the nano-indentation technique. Friction

measurements indicate a low friction coefficient during the leaf falling period. Samples differ in appearance due to leaf contamination. Only the tarnished layer is found to contain very different contents of elements and to be softer than the uncontaminated layers.

Based on the results reported in papers **A–D**, oxide layers are found to be a key issue in wheel–rail adhesion/friction. Detailed research with a special focus on the oxide layer between the wheel and rail surfaces is needed. Paper **E** reports a pin-on-disc study investigating the influence of environmental conditions and iron oxides on wheel–rail friction. The testing samples were pretreated in a climate chamber and X-ray diffraction analysis was performed to detect the iron oxides and rusts created. Pin-on-disc tests were conducted at various relative humidities (RHs) and temperatures. Scanning electron / Focused ion beam microscopy (SEM/FIB) was used to examine the oxygen on the surface and the depth of the oxide layers. The samples containing oxygen were subjected to Raman spectroscopy analysis to determine the specific types of iron oxides/rusts present. The results indicate that the coefficient of friction decreases with increasing RH up to a saturation level; above this level, the coefficient of friction remains low and stable even when the RH increases further. For surfaces with a low friction coefficient, hematite ($\alpha\text{-Fe}_2\text{O}_3$) was the dominant substance on the surface.

3 Discussion

In this chapter, the discussion is structured by the sequence of the research questions and not by the sequence of the appended papers. Some suggestions for the railway industry and for research are made throughout the chapter.

Is it possible to develop a numerical model with which to study the influence of factors such as speed, surface topography, temperature, and plasticity on wheel–rail adhesion?

We developed an adhesion model, based on numerical methods, that can calculate wheel–rail adhesion under dry, water-lubricated, and oil-lubricated conditions. Regarding lubricated contacts (paper **A**), both the adhesion curve (i.e., adhesion coefficient versus creep, keeping speed constant) and the Stribeck curve (i.e., adhesion coefficient versus speed, keeping creep constant) were obtained. At increased speeds, fluids tend to carry more normal load, thus reducing the adhesion coefficient. Surface topography greatly influences the adhesion coefficient. Smoother surfaces can assist the film formation and therefore have a lower adhesion coefficient than do rougher surfaces, which break the film. These findings correspond to results reported in the literature [59,60]. At low speeds ($<21 \text{ m s}^{-1}$), the reduction is not as great as found at high rolling speeds [37,39]. The difference in the absolute value of the adhesion coefficient between the numerical model results and test rig or field measurements depends somewhat on the value of the boundary friction coefficient [67]. The boundary friction coefficient, which depends on, for example, axle load, rail surface conditions, etc., is usually chosen directly from measured values. Better selection of a boundary friction coefficient will give better results. Regarding the dry contact model, paper **B** adds the local contact temperature and local friction coefficient models. These four sub-models cover almost all potential factors affecting wheel–rail adhesion under dry and clean conditions. The four sub-models are coupled and the influential factors need to be studied as a system, as changing one parameter in the system will cause other parameters to change. The influence of the surface topography and the speed on the adhesion coefficient is smaller in dry than in lubricated contacts, though smoother surfaces have a slightly higher adhesion coefficient than do rougher surfaces. The adhesion coefficient decreases with increased speed due to the decreased local friction coefficient and increased contact temperature. The results are in line with test rig and field measurements [37,60,68,69]. However, other local-level factors, such as the contact area, contact temperature, plasticity, and friction coefficient, are found to vary significantly due to surface topography and rolling speed. A smoother surface topography will present a smoother pressure distribution, which will lead to a larger area of high contact temperature. This information can help material researchers examine failure or fatigue due to local stress and temperature as well as those attempting to predict wear.

Plasticity is another essential factor that needs to be included when modelling wheel–rail adhesion. Paper **A** demonstrates that assuming a pure elastic contact significantly changes the results. Especially for high-roughness surfaces, a plastic solution more than doubles

the contact area compared with pure elasticity results. The increased contact area will also greatly influence the fluid lubrication and contact temperature. Although the plasticity considered in papers **A** and **B** is simplified, it leads to results that differ significantly from those of a pure elasticity model.

In the numerical modelling, all results are obtained from one pair of smooth surfaces and two pairs of real measured 3D surfaces. The results obtained from low-roughness surfaces are close to those from the generated smooth surfaces under lubricated conditions. According to Lundmark [29], a roughness value of 1 μm is fairly typical of a heavy-haul line after the first one and a half days of traffic on newly ground surfaces. Therefore, regularly used rails without severe wear can be nearly as smooth as or even smoother than the low-roughness surfaces used here (i.e., R_a values of 4.11 μm and 2.65 μm for the wheel and rail, respectively). Those regularly used rails tend to have more adhesion loss problems than do very rough surfaces; for example, sand-damaged surfaces (called high-roughness surfaces in this thesis: R_a values of 12.45 and 20.38 μm for the wheel and rail, respectively) when water or oil is present.

The representation of the surface topography, which affects contact area and contact pressure, depends on the measurement resolution and the simulation resolution. In the thesis, the surface pairs are measured using a stylus machine with an interval of 0.01 mm in both the x and y directions. In the computer simulation based on the numerical model, the measurement data are processed to a low resolution due to the computation time. The mesh grids used in the simulation are 38×38 elements, each element being $0.4 \times 0.4 \text{ mm}^2$ in size. For the generated smooth and low-roughness surfaces, the mesh grids satisfactorily represent the surface topography: since the waviness is great, the numerical error is comparatively small. However, for the high-roughness surfaces, the mesh grids supply inadequate resolution, since the surface waviness is fairly small. As a result, the mesh grids cannot represent the whole surface topography in detail. The results obtained for the high-roughness surfaces may contain comparatively large errors and can be used for comparative purposes only.

Is it possible to experimentally simulate the lubricated wheel–rail contact in the laboratory environment; if so, how do experiments compare with the real situation?

A ball-on-disc-based investigation was carried out to simulate a wheel–rail contact in a laboratory environment. Based on a calculated lambda value, the experimental and the real wheel–rail contacts were compared. The comparison results indicate that the lubrication regime of the oil-lubricated contact is mixed lubrication to elasto-hydrodynamic lubrication, depending on the speed and surface roughness; however, in the water-lubricated contact, the regime is entirely boundary lubrication. Experimental results indicate similar lubrication regimes when oil is used as the lubricant. Under oil-lubricated conditions, surface topography is important only at low speed. When the rolling speed is high, the influence of the surface topography and lubricant temperature on the adhesion coefficient is negligible. However, under water-lubricated conditions, high water temperature tends to increase the adhesion coefficient on rough surfaces, in line with the results reported in the literature [39,59]. It can be a quite practical

suggestion for railway industry to combat low adhesion. Regarding the smooth surfaces, water gives an extremely low adhesion coefficient. Surface topography measurements also indicate fewer and thinner surface scratches on a water-lubricated than an oil-lubricated test disc. These phenomena cannot be explained by classic tribology theory in which surface oxidation may be taking place.

What is the mechanism of adhesion loss due to water and oil?

Water and oil are very common contaminants, both of which are known to reduce adhesion between the wheel and rail. Paper **A** found that oil could reduce the adhesion coefficient much more than water could when the speed was increased within a low speed range. The fluid load capacity is inversely proportional to the adhesion coefficient. The load carried by water is much less than that carried by oil, though both cases are in the mixed lubrication regime. This is because that the viscosity of water is only 0.1% of that of oil. These results are in line with the experimental findings from paper **C** regarding rough discs in water- and oil-lubricated contacts and from other experimental work [37,56]. According to the theoretical results, the effect of water is mainly to reduce the adhesion force (one part of the frictional force); the hydrodynamic effect of the water film between two surfaces can be neglected. However, under water-lubricated conditions, the smooth disc described in paper **C** has an extremely low adhesion coefficient that cannot be explained by the theoretical calculations. This could be because the squeeze effect of the rolling was not considered in the simulation; this effect needs to be considered, as the wheel–rail contact is a non-steady-state contact. Another, more likely explanation is that a tribo-film forms on the smooth-disc surface which cannot be simulated in the adhesion model. Beagley and Pritchard [42] investigated the influence of water and oil using scaled laboratory rigs. They found that water could cause only a very small reduction in the adhesion coefficient on stainless steels, but a small amount of water mixed with oil or wear debris could reduce the adhesion substantially. Nakahara et al. [45] observed and analysed the generation and influence of oxide layers on a water-lubricated contact. Therefore, compared with an oil-lubricated contact, whose behaviour can be predicted by classic lubrication theory, a water-lubricated contact is significantly affected by tribo-films, such as oxide layers; this effect is transient and difficult to predict or control. The real situation on rail surfaces in the field is even more complicated, as the wheel–rail contact can be exposed to various contaminants due to the system’s open nature. Measurements made from locomotives [23] also indicate large adhesion variations when rails are wet. Rail surface conditions can vary significantly due to the presence of wear debris, iron oxides, or other contaminants, even though they appear simply to be “wet” to the naked eye. As the removal of such surface contaminants by running wheels depends on the speed, axle load, and slip, the adhesion recovery can vary. Moreover, the amount of water also significantly influences the adhesion reduction. As Beagley and Pritchard [42] pointed out, a large amount of water reduces adhesion only slightly, because it can clean away contaminants, while a small amount of water can mix with other contaminants to reduce the adhesion significantly.

How do leaves on rails reduce the friction coefficient? What is the key factor in this issue?

Paper **D** investigates leaf contamination on railhead surfaces by comparing different rail samples cut on five occasions over a year. Surface chemistry results indicate that the tarnished rail sample taken in October differs greatly in elemental content and depth profile from the samples taken on other occasions. The tarnished layer is much softer than the non-tarnished layer of the same running band. These facts indicate that the tarnished layer results from a chemical reaction between the leaves and bulk materials, and that the chemical reaction occurs from the surface to a depth of several microns.

According to Zhao et al. [70], the oxide coating structure can be divided into three sub-layers. The superficial sub-layer is the friction-reducing layer that plays the key role in reducing the friction of steel. We performed an additional study by measuring the thickness of the friction-reducing layer, and obtained very interesting results. The measured friction coefficient is inversely proportional to the thickness of the friction-reducing oxide layer, i.e., the greater the thickness, the lower the friction coefficient. The tarnished-layer sample has the thickest friction-reducing oxide layer of all the samples. Moreover, two other samples taken in October, one with leaf residue and the other with no visible contamination, also have much thicker friction-reducing oxide layers than do samples taken on other occasions, though these oxide layers are much thinner than the tarnished layer. This fact indicates that all three samples were contaminated with leaves, though they differed in appearance, the appearance being related to the degree of leaf contamination.

The most common way to clean rails to recover adhesion is to use sand [53]. Due to the side effect of increasing wear, parameters such as sand particle hardness and size need to be optimized. Other rail cleaning methods are high-pressure water jetting or high-powered laser units [54]. Rail re-profiling is also sometimes used to recover adhesion. The success of these adhesion recovery measures depends on the amount of contaminated material removed. The investigation carried out here suggests that removing the friction-reducing oxide layer is important for adhesion recovery. In addition, any leaves on the lines (on the tracks and nearby) need to be removed as soon as possible before they are crushed by running wheels, becoming rail contaminants. When leaves are already crushed and left on rail surfaces, the leaf layers must be removed before they fully react with bulk material and become tarnished layers.

How do environmental conditions and iron oxides influence the friction and adhesion?

The effects of iron oxide and environmental conditions on the friction coefficient between the wheel and rail are examined in paper **E**. This study is motivated partially by the importance of the environmental conditions due to the open nature of the wheel–rail system, and partially by previous investigations. The iron oxides were prepared as described in the literature [42]. However, akaganeite (β - $\text{Fe}_2\text{O}_3 \cdot \text{H}_2\text{O}$), which is suggested to be a very important substance reducing the friction coefficient [2,71], was not found after the exposure in the present research. This may be because the rail materials differed or because different parts of the rail materials were used. Heavy rust layers, which were pre-created using NaCl, can keep the friction coefficient high, independent of temperature or the presence of a small amount of water. Pre-created thin rust does not

show significant difference in the friction coefficient compared with samples without such rust, because the pure sliding under high pressure from the pin-on-disc rig removes the pre-created rust layer very quickly. After removal of the pre-created rust layers, the iron oxide is generated and then breaks, independent of the pre-created layers. In the plot of friction versus RH shown in Figure 3.1, a transition is evident at approximately 65% RH for thin rust samples— a phenomenon also found by other researchers [48,72]. Liew [72] reported such a transition between 50% and 60% RH using the same test rig. Hayashi et al. [48] also identified transitions taking place between 35% and 63% RH. When the speed is not very high, the friction coefficient is suggested to be a function of the RH. This relationship can be applied in studies of wear and rolling contact fatigue, for example, where a constant friction coefficient is usually assumed under “dry” conditions. Moreover, we find that at low temperatures, a small increase in the amount of water vapour in the air will significantly reduce the friction coefficient. This explains the increase in low-friction problems observed in the winter on Swedish railway lines.

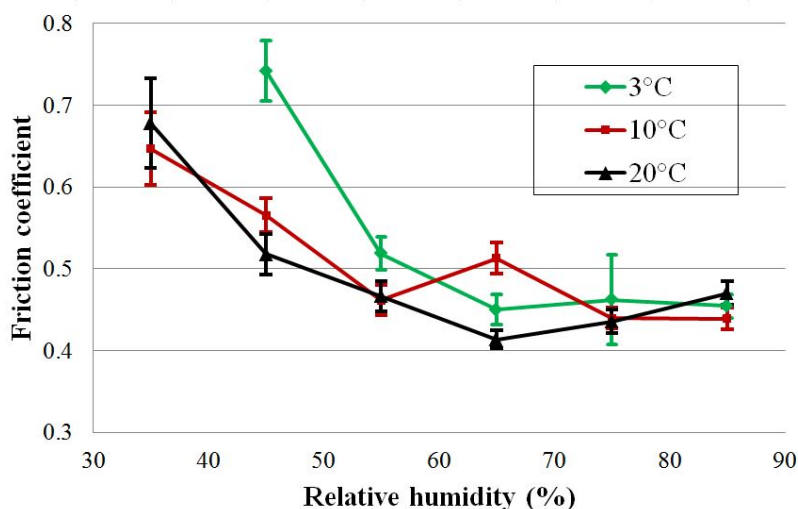


Figure 3.1. Friction coefficient plotted versus RH for thin rust samples at three temperatures.

Surface chemistry analysis reveals no oxygen on the surfaces when the RH is low, while much of the oxygen is found in the form of hematite ($\alpha\text{-Fe}_2\text{O}_3$) when RH is high. The mechanism of the friction behaviour due to RH is as follows: in the first phase, the friction coefficient decreases with increased RH due to the effect of boundary lubrication by the water molecule film; in the second phase, the friction coefficient stabilizes at a low level because the increased amount of water is able to keep the hematite on the surface, weakening the effect of the boundary lubrication [73]. Therefore, the change in the friction coefficient is a trade-off between the water molecule film and hematite generation. Interestingly, the hematite generated on the surfaces helps maintain the friction coefficient between the wheel and rail, preventing it from declining further in a humid environment such as that found on tracks near the sea. However, since the oxidation process is usually transient and difficult to predict in the field, it is difficult to replicate the same conditions in the laboratory [36].

4 Conclusions

The thesis allows several main conclusions to be drawn:

- A numerical model was developed that can calculate wheel–rail adhesion under dry, water-lubricated, and oil-lubricated conditions. Surface topography has a larger impact on lubricated than on dry contacts. Increased speed reduces the adhesion coefficient under all conditions, though for different reasons. The plastic deformation of asperities is crucial as it drastically affects the contact area. In dry contacts, increased speed will increase the contact temperature. Surface topography influences contact temperature at the local level.
- A ball-on-disc test rig was used to simulate wheel–rail contact under lubricated conditions. Calculations based on the specific film thickness can be useful when comparing scaled laboratory experiments with real situations in terms of the lubrication regime. The test rig results indicate that water can have an extremely low adhesion coefficient.
- The results of the computer simulation and the ball-on-disc test indicate that the presence of oil reduces the adhesion coefficient, since oil can carry the normal load due to its high viscosity. The adhesion reduction due to the presence of water depends greatly on the surface topography, water temperature, and surface oxidation.
- Field test results indicate that leaf contamination can reduce the friction coefficient due to the chemical reaction between the leaves and bulk materials. The thickness of the surface oxide layer is closely related to the friction coefficient.
- Pin-on-disc experiments demonstrate that the friction coefficient decreases with increasing RH up to a saturation level, because water molecules act as a lubricating film. Above this level, the coefficient of friction remains stable and low when the RH increases, due to a trade-off between the water molecule film and the hematite on the surface. Temperature significantly affects friction: especially when the temperature is low, a small change in absolute humidity (i.e., the amount of water in air) will greatly reduce the friction coefficient.

5 Future work

This thesis deals with the adhesion loss mechanism under various contaminants. Some productive avenues for future research are suggested by the author:

In adhesion modelling, plasticity could be further considered by including the work hardening process of asperities in the model and comparing the results with those of the present model to determine key parameters. Another interesting extension would be to include newly ground rail surfaces in the numerical model. Newly ground rail surfaces have certain surface textures that may greatly affect adhesion and wear at an initial stage. As a physical model is lacking, the friction coefficient needs to be measured under various conditions to produce comprehensive data on the friction coefficient that can be used for all levels of modelling.

Regarding third-body layers, which are not well understood, research should concentrate on studying the relevant mechanisms experimentally. Surface chemical analysis is an efficient way to investigate these poorly understood third-body layers and identify the key substances in them. The influence of the oxide layer merits considerable attention, since it can be mixed with other third bodies and is fairly transient. First, investigating the oxidation on rails in the field would advance the study of the real oxidation process. Second, the depth of the oxide layer and the friction coefficient should be quantitatively analysed. Third, the oxide layer needs to be considered together with mixtures of contaminants such as oil, water, and sand. Adhesion modelling of these third-body layers, which are not well understood, is difficult and usually needs to be combined with experimental results.

For tribologists, the mechanism of adhesion loss due to various contaminants is of great interest. For modellers of vehicle dynamics, the main focus of adhesion research is to implement key factors affecting wheel–rail adhesion in a fast contact model. Therefore, the mechanism of the adhesion loss needs to be investigated so the relationships between the influential factors and the adhesion coefficient can be developed. Then these relationships need to be simplified so they can be incorporated into the fast contact model and, furthermore, into multi-body vehicle dynamic simulation. The efforts of both tribologists and vehicle dynamic modellers are needed to advance this work.

Appendix I: A simplified model for calculating the required adhesion coefficient

The relationship between acceleration/deceleration and the adhesion coefficient can be explained by a simplified model.

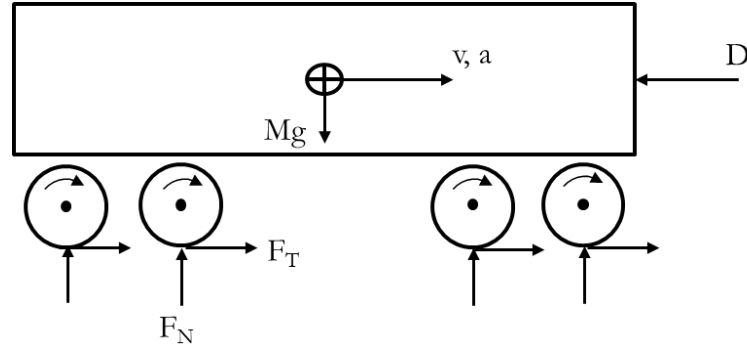


Figure A.1. Schematic of a single vehicle with propulsion.

As shown in Figure A.1, assume a single vehicle running with acceleration, a , whose load is equally distributed between the axles and wheels, all of which are powered. The vehicle is subject to gravity, Mg , and the running resistance, D . F_N is the normal force and F_T is the adhesion for each axle. The following equations can be obtained:

$$\sum F_N = Mg \quad (4.1)$$

$$F_T = \mu_a F_N \quad (4.2)$$

$$F_a = \sum F_T = \mu_a \sum F_N = \mu_a Mg \quad (4.3)$$

$$F_a = Ma + D \quad (4.4)$$

where μ_a is the adhesion coefficient and F_a is the total adhesion. Equations (4.3) and (4.4) give:

$$\mu_a = a / g + D / Mg \quad (4.5)$$

According to Jacobsson [35], the measured acceleration is approximately 1.5 m s^{-2} for a metro vehicle, so the required adhesion coefficient should be as least 0.15 based on this simplified model.

References

- [1] R. Lewis, U. Olofsson, eds., *Wheel-rail interface handbook*, Woodhead publishing limited, 2009.
- [2] J. Suzumura, Y. Sone, A. Ishizaki, D. Yamashita, Y. Nakajima, M. Ishida, In situ X-ray analytical study on the alteration process of iron oxide layers at the railhead surface while under railway traffic, *Wear*. 271 (2011) 47–53.
- [3] E. Andersson, M. Berg, S. Stichel, *Rail vehicle dynamics*, Stockholm, 2007.
- [4] Y. Zhu, *Adhesion in the wheel – rail contact under contaminated conditions*, Licentiate thesis, KTH Royal Institute of Technology, 2011.
- [5] V.A. Profillidis, *Railway management and engineering*, Third edit, Ashgate Publishing Limited, Hampshire, England, 2006.
- [6] BS 5892-3: 1992. *Railway rolling stock materials — Part 3: specification for monobloc wheels for traction and trailing stock*, (1992).
- [7] U. Olofsson, T. Telliskivi, *Wear*, plastic deformation and friction of two rail steels—a full-scale test and a laboratory study, *Wear*. 254 (2003) 80–93.
- [8] R. Lewis, U. Olofsson, Mapping rail wear regimes and transitions, *Wear*. 257 (2004) 721–729.
- [9] R. Nilsson, *On wear in rolling/sliding contacts*, Doctoral thesis, KTH Royal Institute of Technology, 2005.
- [10] M.B. Marshall, R. Lewis, R.S. Dwyer-Joyce, U. Olofsson, S. Björklund, Experimental Characterization of Wheel-Rail Contact Patch Evolution, *Journal of Tribology*. 128 (2006) 493.
- [11] S. Björklund, S. Andersson, A Numerical Method for Real Elastic Contacts Subjected to Normal and Tangential Loading, *Wear*. 179 (1994) 117–122.
- [12] S. Lin, T. Tabata, H. Doi, H. Chen, J. Nakahashi, M. Kuzuta, et al., Basic study of contact geometry on turnout by using full size wheelset model, in: S. Iwnicki, R. Goodall, T.X. Mei (Eds.), *22nd International Symposium on Dynamics of Vehicles on Roads and Tracks*, Manchester, UK, 2011.
- [13] C. Hung, H. Doi, K. Nunotani, S. Lin, Experiments to measure stress with the wheel/rail contact using embedded FBG sensors, in: *9th International Conference on Contact Mechanics and Wear of Rail/Wheel Systems*, Chengdu, China, 2012: pp. 752–757.
- [14] E.A.H. Vollebregt, *User guide for CONTACT*, Vollebregt & Kalker’s rolling and sliding contact model., Delft, The Netherlands, 2012.

- [15] T. Telliskivi, U. Olofsson, Contact mechanics analysis of measured wheel-rail profiles using the finite element method, *Proceedings of the Institution of Mechanical Engineers, Part F: Journal of Rail and Rapid Transit.* 215 (2001) 65–72.
- [16] BS EN 13144:2003, *Metallic and Other Inorganic Coatings – Method for Quantitative Measurement of Adhesion by Tensile Test.* London: British Standards Institution.
- [17] 4624:2003 BS EN ISO, *Paints and Varnishes – Pull-off Test for Adhesion.* London: British Standards Institution.
- [18] D.I. Fletcher, S. Lewis, Creep curve measurement to support wear and adhesion modelling, using a continuously variable creep twin disc machine, *Wear.* 298-299 (2013) 57–65.
- [19] S.R. Lewis, *Measurement, Control and Enhancement of Friction/Traction in a Simulated Wheel/Rail Contact*, Doctoral thesis, University of Sheffield, 2011.
- [20] I.M. Hutchings, *Tribology: friction and wear of engineering materials*, Edward Arnold, 1992.
- [21] N.P. Suh, *Tribophysics*, Englewood Cliffs, NJ, USA, 1986.
- [22] J. Kalker, Wheel-rail rolling contact theory, *Wear.* 144 (1991) 243–261.
- [23] O. Polach, Creep forces in simulations of traction vehicles running on adhesion limit, *Wear.* 258 (2005) 992–1000.
- [24] E. Andersson, M. Berg, *Spårfordonsteknik Rail Vehicle Technology*, KTH,, Stockholm, n.d.
- [25] H. Harrison, T. McCanney, J. Cotter, Recent developments in coefficient of friction measurements at the rail/wheel interface, *Wear.* 253 (2002) 114–123.
- [26] R. Lewis, S.R. Lewis, Y. Zhu, S. Abbasi, U. Olofsson, The modification of a slip resistance meter for measurement of railhead adhesion, *Proceedings of the Institution of Mechanical Engineers, Part F: Journal of Rail and Rapid Transit.* 227 (2012) 196–200.
- [27] S. Björklund, *Elastic contacts between rough surfaces*, Doctoral thesis, Royal Institute of Technology KTH, 1995.
- [28] J. Sundh, *On wear transitions in the wheel-rail contact*, Doctoral thesis, Royal Institute of Technology KTH, 2009.
- [29] J. Lundmark, E. Höglund, B. Prakash, Running-in behaviour of rail and wheel contacting surfaces, *Proceedings of the International Conference on Tribology*, 20-22 Sep. 2006, Parma, Italy.
- [30] T.R. Thomas, *Rough surfaces*, 2nd editio, Imperial college press, 1999.

- [31] C. Esveld, L. Gronskov, MINIPROF wheel and rail profile measurement, in: Proceedings of 2nd Miniconference on Contact Mechanics and Wear of Rail/Wheel Systems, Budapest, Hungary, 1996.
- [32] P. Dings, M. Dittrich, Roughness on Dutch railway wheels and rails, *Journal of Sound and Vibration*. 193 (1996) 103–112.
- [33] O. Arias-Cuevas, Z. Li, R. Lewis, A laboratory investigation on the influence of the particle size and slip during sanding on the adhesion and wear in the wheel–rail contact, *Wear*. 271 (2011) 14–24.
- [34] O. Arias-Cuevas, Low adhesion in the wheel-rail contact, Doctoral thesis, Delft University of Technology, 2010.
- [35] M. Jacobsson, SL technical report: Teknikforum Halt Spår, 1 (2011) 1–59.
- [36] R. Lewis, R.S. Dwyer-Joyce, S.R. Lewis, C. Hardwick, E. a. Gallardo-Hernández, Tribology of the wheel-rail contact: The effect of third body materials, *International Journal of Railway Technology*. 1 (2012) 167–194.
- [37] W. Zhang, J. Chen, X. Wu, X. Jin, Wheel/rail adhesion and analysis by using full scale roller rig, *Wear*. 253 (2002) 82–88.
- [38] T. Ohyama, Tribological studies on adhesion phenomena and rail at high speeds, 144 (1991) 263–275.
- [39] H. Chen, T. Ban, M. Ishida, T. Nakahara, Experimental investigation of influential factors on adhesion between wheel and rail under wet conditions, *Wear*. 265 (2008) 1504–1511.
- [40] R. Lewis, E. a. Gallardo-Hernandez, T. Hilton, T. Armitage, Effect of oil and water mixtures on adhesion in the wheel/rail contact, *Proceedings of the Institution of Mechanical Engineers, Part F: Journal of Rail and Rapid Transit*. 223 (2009) 275–283.
- [41] W.J. Wang, H.F. Zhang, H.Y. Wang, Q.Y. Liu, M.H. Zhu, Study on the adhesion behavior of wheel/rail under oil, water and sanding conditions, *Wear*. 271 (2011) 2693–2698.
- [42] T. Beagley, C. Pritchard, Wheel/rail adhesion—the overriding influence of water, *Wear*. 35 (1975) 299–313.
- [43] T.M. Beagley, I.J. McEwen, C. Pritchard, Wheel/rail adhesion—Boundary lubrication by oily fluids, *Wear*. 31 (1975) 77–88.
- [44] T. Beagley, I. McEwen, C. Pritchard, Wheel/rail adhesion—the influence of railhead debris, *Wear*. 33 (1975) 141–152.
- [45] T. Nakahara, K.-S. Baek, H. Chen, M. Ishida, Relationship between surface oxide layer and transient traction characteristics for two steel rollers under unlubricated and water lubricated conditions, *Wear*. 271 (2011) 25–31.

- [46] K. Ohno, Y. Ogawa, RTRI Rep. No. A-83-70, 1983, In Japanese, (n.d.).
- [47] U. Olofsson, K. Sundvall, Influence of leaf, humidity and applied lubrication on friction in the wheel-rail contact: pin-on-disc experiments, Proceedings of the Institution of Mechanical Engineers, Part F: Journal of Rail and Rapid Transit. 218 (2004) 235–242.
- [48] O. Hayashi, T. Nomura, K. Nagase, Influence of atmospheric conditions upon adhesion between rails and running wheels, Trans. Jap. Soc. Mech. Engrs, Part C. (1997).
- [49] D.F. Moore, Principles and applications of tribology, Elsevier, Amsterdam, 1998.
- [50] C. Fulford, Review of low adhesion research, Report Published by the Rail Safety and Standards Board(2004).
- [51] L. Forslöv, Wheel slip due to leaf contamination, Borlänge, Sweden, 1996.
- [52] Managing low adhesion, UK, 2001.
- [53] O. Arias-Cuevas, Z. Li, Field investigations into the adhesion recovery in leaf-contaminated wheel-rail contacts with locomotive sanders, Proceedings of the Institution of Mechanical Engineers, Part F: Journal of Rail and Rapid Transit. 225 (2011) 443–456.
- [54] U. Olofsson, A multi-layer model of low adhesion between railway wheel and rail, Proceedings of the Institution of Mechanical Engineers, Part F: Journal of Rail and Rapid Transit. 221 (2007) 385–389.
- [55] Z. Li, O. Arias-Cuevas, R. Lewis, E. a. Gallardo-Hernández, Rolling–Sliding Laboratory Tests of Friction Modifiers in Leaf Contaminated Wheel–Rail Contacts, Tribology Letters. 33 (2008) 97–109.
- [56] E. A. Gallardo-Hernandez, R. Lewis, Twin disc assessment of wheel/rail adhesion, Wear. 265 (2008) 1309–1316.
- [57] P.M. Cann, The “leaves on the line” problem—a study of leaf residue film formation and lubricity under laboratory test conditions, Tribology Letters. 24 (2006) 151–158.
- [58] H. Chen, T. Ban, M. Ishida, T. Nakahara, Adhesion between rail/wheel under water lubricated contact, Wear. 253 (2002) 75–81.
- [59] H. Chen, M. Ishida, T. Nakahara, Analysis of adhesion under wet conditions for three-dimensional contact considering surface roughness, Wear. 258 (2005) 1209–1216.
- [60] C. Tomberger, P. Dietmaier, W. Sextro, K. Six, Friction in wheel–rail contact: A model comprising interfacial fluids, surface roughness and temperature, Wear. 271 (2011) 2–12.

- [61] A. Meierhofer, C. Hardwick, R. Lewis, K. Sixa, P. Dietmaier, Third body layer-experimental results and a model describing its influence on the traction coefficient, in: Proceedings of 9th International Conference on Contact Mechanics and Wear of Rail/wheel System, Chengdu, China, 2012.
- [62] J. Kalousek, E. Magel, Modifying and managing friction, in: Railway Track & Structures, 1997: pp. 5–6.
- [63] D.T. Eadie, J. Kalousek, K.C. Chiddick, The role of high positive friction (HPF) modifier in the control of short pitch corrugations and related phenomena, *Wear*. 253 (2002) 185–192.
- [64] O. Arias-Cuevas, Z. Li, Field investigations into the performance of magnetic track brakes of an electrical multiple unit against slippery tracks. Part 1: Adhesion improvement, Proceedings of the Institution of Mechanical Engineers, Part F: Journal of Rail and Rapid Transit. 225 (2011) 613–636.
- [65] V.L. Popov, S.G. Psakhie, E. V Shilko, A.I. Dmitriev, K. Knothe, F. Bucher, et al., Friction coefficient in “rail— wheel” -contact as a function of material and loading parameters, 3 (2002) 1–8.
- [66] K. Knothe, S. Liebelt, Determination of temperatures for sliding contact with applications for wheel-rail systems, *Wear*. 189 (1995) 91–99.
- [67] H. Chen, M. Ishida, A. Namura, K.-S. Baek, T. Nakahara, B. Leban, et al., Estimation of wheel/rail adhesion coefficient under wet condition with measured boundary friction coefficient and real contact area, *Wear*. 271 (2011) 32–39.
- [68] J. Lundmark, E. Kassfeldt, J. Hardell, B. Prakash, The influence of initial surface topography on tribological performance of the wheel/rail interface during rolling/sliding conditions, Proceedings of the Institution of Mechanical Engineers, Part F: Journal of Rail and Rapid Transit. 223 (2009) 181–187.
- [69] W.J. Wang, P. Shen, J.H. Song, J. Guo, Q.Y. Liu, X.S. Jin, Experimental study on adhesion behavior of wheel/rail under dry and water conditions, *Wear*. 271 (2011) 2699–2705.
- [70] Y. Zhao, J. Liu, L. Zheng, The oxide film and oxide coating on steels under boundary lubrication, in: The 16th Leeds-Lyon Symposium on Tribology, 1989: p. 305.
- [71] Y. Sone, J. Suzumura, T. Ban, F. Aoki, M. Ishida, Possibility of in situ spectroscopic analysis for iron rust on the running band of rail, *Wear*. 265 (2008) 1396–1401.
- [72] W.Y.H. Liew, Effect of relative humidity on the unlubricated wear of metals, *Wear*. 260 (2006) 720–727.
- [73] D. Godfrey, Iron oxides and rust (hydrated iron oxides) in tribology, *Journal of the Society of Tribologists and Lubrication Engineers*. 55 (1999) 33–37.

